STEM CELLS TRANSLATIONAL MEDICINE®

TISSUE-SPECIFIC PROGENITOR AND STEM CELLS

Pre-Exposure of Human Adipose Mesenchymal Stem Cells to Soluble Factors Enhances Their Homing to Brain Cancer

CHRIS L. SMITH,[a,b] KAISORN L. CHAICHANA,[a] YOUNG M. LEE,[a] BENJAMIN LIN,[b] KEVIN M. STANKO,[a] THOMAS O'DONNELL,[a] SAKSHAM GUPTA,[b] SAGAR R. SHAH,[a,b] JOANNE WANG,[a] OLINDI WIJESEKERA,[a] MICHAEL DELANNOY,[b] ANDRE LEVCHENKO,[b] ALFREDO QUIÑONES-HINOJOSA[a]

Key Words. Adipose • Bone marrow • Brain tumor • Glioblastoma • Homing • Mesenchymal stem cells

Departments of [a]Neurosurgery and [b]Biomedical Engineering, Johns Hopkins University School of Medicine, Baltimore, Maryland, USA

Correspondence: Alfredo Quiñones-Hinojosa, M.D., Department of Neurosurgery, Johns Hopkins Hospital, Johns Hopkins University, CRB II, 1550 Orleans Street, Room 247, Baltimore, Maryland 21231, USA. Telephone: 410-502-2906; E-Mail: aquinon2@jhmi.edu; or Andre Levchenko, Ph.D., Department of Biomedical Engineering, Yale University, P.O. Box 208260, New Haven, Connecticut 06520, USA. Telephone: 410-949-5944; E-mail: andre.levchenko@yale.edu

Received July 27, 2014; accepted for publication December 3, 2014; first published online in SCTM *Express* February 2, 2015.

1066-5099/2015/$20.00/0

http://dx.doi.org/10.5966/sctm.2014-0149

ABSTRACT

Recent research advances have established mesenchymal stem cells (MSCs) as a promising vehicle for therapeutic delivery. Their intrinsic tropism for brain injury and brain tumors, their lack of immunogenicity, and their ability to breach the blood-brain barrier make these cells an attractive potential treatment of brain disorders, including brain cancer. Despite these advantages, the efficiency of MSC homing to the brain has been limited in commonly used protocols, hindering the feasibility of such therapies. In the present study, we report a reproducible, comprehensive, cell culture-based approach to enhance human adipose-derived MSC (hAMSC) engraftment to brain tumors. We used micro- and nanotechnological tools to systematically model several steps in the putative homing process. By pre-exposing hAMSCs to glioma-conditioned media and the extracellular matrix proteins fibronectin and laminin, we achieved significant enhancements of the individual homing steps in vitro. This homing was confirmed in an in vivo rodent model of brain cancer. This comprehensive, cell-conditioning approach provides a novel method to enhance stem cell homing to gliomas and, potentially, other neurological disorders. STEM CELLS TRANSLATIONAL MEDICINE *2015;4:239–251*

INTRODUCTION

Adult stem cells, in particular, mesenchymal stem cells (MSCs), have garnered significant attention for their potential to treat a variety of pathologic entities, including neurological disorders [1–8]. MSCs possess an intrinsic tropism for the sites of neurological pathologies, including infarcted tissue and tumors [1–8], and have the ability to bypass the blood-brain barrier (BBB) [9]. MSCs can also reside within the bloodstream as pericytes and play an important role in responding to stress and inflammation, homing primarily to sites of injury such as inflamed or broken blood vessels to participate in regeneration. These cells also avoid the ethical concerns of embryonic sources [3, 10, 11] are relatively easy to isolate, and are nonimmunogenic [3]. Despite these advantages, a major challenge to potential therapies resides in the efficiency of MSCs homing to certain locations [3, 12, 13]. In neurological conditions, less than 1% of systemically injected MSCs will engraft at sites of brain pathologies [3, 13, 14]. The presence of mis-targeted MSCs decreases their overall therapeutic efficacy and can lead to unwanted side effects, thus compromising the commonly used systemic delivery methods [3, 12]. Previous work has shown that nascent MSCs have a therapeutic effect on homing to brain tumors [15]. Thus, by increasing the percentage of MSCs localized to the brain, their therapeutic effects could be augmented further. Methods that enhance MSC trafficking to the brain could offer significant value to emerging stem cell-based therapies.

The interaction between MSCs and the host tissues depends on adaptive interactions between the stem and tissue cells. We thus hypothesized that the homing of MSCs might be improved by preincubating these cells under conditions that mimic the local microenvironment of the tissue of interest. To test this hypothesis, in the present study, we used a glioma brain cancer model to test human adipose-derived MSC (hAMSC) homing, a multistep process that bears similarity to homing of other cell types, including leukocyte homing during inflammation (Fig. 1) [2, 3, 16]. Previous studies have shown that the extracellular matrix directs the crosstalk between receptors on MSCs such as platelet-derived growth factor receptor (PDGFR)-β and $\alpha5\beta1$-integrin, which control the migration of MSCs. Specifically, fibronectin has been shown to induce PDGFR-β signaling in an $\alpha5\beta1$-integrin-dependent manner [17]. Laminin has

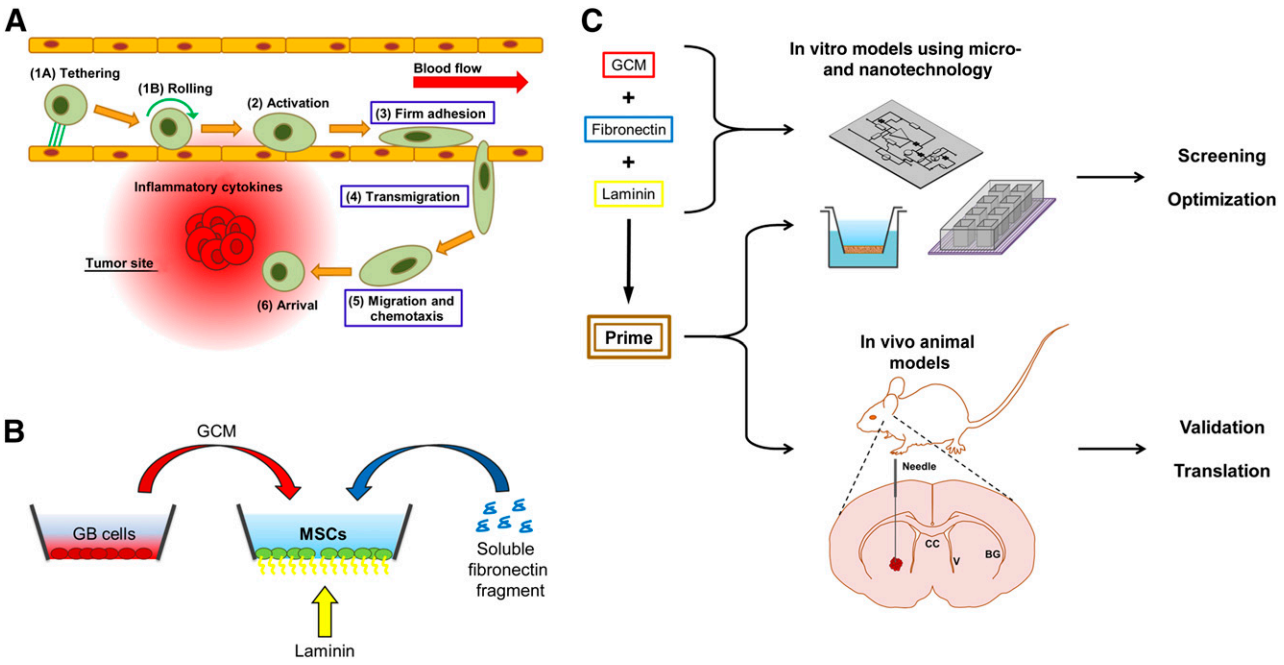

Figure 1. Comprehensive, cell culture-based enhancement of stem cell homing. **(A):** Putative MSC homing mechanisms. This study examined steps 3, firm adhesion, 4, transmigration, and 5, migration and chemotaxis. (Adapted from Sackstein et al. [16].) **(B):** The protocol for environmental perturbations of human adipocyte-derived MSCs (hAMSCs). Before the experiments, hAMSCs were grown on laminin for 3 weeks and/or exposed to GCM and/or soluble fibronectin (FN) fragments. **(C):** Experimental paradigm for analysis of hAMSC homing. Each perturbation (GCM, FN, and laminin) was tested individually using in vitro models for screening and optimization. The treatments were combined in a single protocol denoted "prime." This combined protocol was tested in vitro and validated in vivo. Abbreviations: BG, basal ganglia; CC, corpus callosum; GB, glioblastoma; GCM, glioma-conditioned medium; MSC, mesenchymal stem cell; V, ventricle.

also been shown to produce an increase in the activity of PDGFR-β in the presence of PDGF-BB, also increasing the migration of MSCs. Fibronectin has also been identified as a key factor in human serum to recruit MSCs for regenerative purposes such as for the subchondral migration of MSCs into cartilage defects after the occurrence of microfractures in vivo [18]. However, no studies to date have investigated the feasibility of using preconditioning to fibronectin, laminin, and glioma-conditioned media, both alone and in combination, to improve the tumor-tropism ability of MSCs. By pre-exposing (i.e., "priming") human-derived MSCs to glioma-conditioned medium (GCM) and the extracellular matrix (ECM) proteins fibronectin (FN) and laminin (LM) in cell culture, we were able to enhance the multiple steps involved in MSC homing, including integration with vascular endothelium and directed migration within the tumor-conditioned microenvironment [2, 3].

Materials and Methods

Experimental Design

Our experimental design is highlighted in Figure 1, illustrating the multistep process of homing established for many cell types [2, 3, 16]. As diagramed in steps 1–3 of Figure 1A, the initial steps of the putative homing process involve interactions between hAMSCs and the vascular endothelium. The cells circulating in the bloodstream first attach, or "tether" (step 1A), to the wall of a vessel. After the initial attachment, the cells roll along the vessel wall near the site of injury (step 1B) and then firmly adhere to the vascular endothelium (step 3). After adhesion, the cells must transmigrate through the vascular endothelium, crossing the BBB (step 4; Fig. 1A). After transmigration, the cells need to effectively migrate toward the tumor (step 5; Fig. 1A). The aim of our analysis was to assess whether pretreating hAMSCs with different environmental conditions (GCM, FN, and/or LM) that mimic the distinct microenvironments encountered in the multiple steps of the homing process (Fig. 1B) can facilitate or augment the overall homing process both in vitro and in vivo (Fig. 1C).

Cells

We maintained hAMSCs, obtained from both commercial sources and primary patient tumors (with permission from the Johns Hopkins institutional review board), for a maximum of 12 passages. hAMSCs (R7788-115; Invitrogen, Carlsbad, CA, http://www.invitrogen.com) were cultured in MesenPRO complete medium with added antibiotic/antimycotic (1%, Invitrogen), GlutaMAX (1%, Gibco, Grand Island, NY, http://www.invitrogen.com). MesenPRO was composed of 1 vial of MesenPRO RS growth supplement (Gibco) and MesenPRO RS basal medium (Gibco). The growth supplement contained approximately 2% fetal bovine serum (FBS). In previous work, we verified the ability of primary and commercial hAMSCs to generate multiple lineages and express established MSC markers [19].

U87 MG human glioblastoma (GBM) cells were obtained from Sigma-Aldrich (89081402; St. Louis, MO, http://www.sigmaaldrich.com). Primary intraoperative human fetal astrocytes (sample F60) and GBM cells (sample 549) were obtained from intraoperative tissue from our patients (approved by the Johns Hopkins institutional review board). All astrocytes and GBM cells were cultured in flasks coated with LM (1 μg/cm^2; Sigma-Aldrich) with the following medium composition: Dulbecco's modified Eagle's

medium (DMEM)/F12 (11330-032; Invitrogen) with 1% antibiotic/antimycotic, 2% B27 (Invitrogen), 20 ng/ml human fibroblast growth factor-basic (PeproTech, Rocky Hill, NJ, http://www.peprotech.com), and 20 ng/ml human epidermal growth factor (PeproTech).

Human brain microvascular endothelial cells (hBMECs; a gift of the Piotr Walczak Laboratory) were isolated and immortalized using established protocols [20]. hBMECs were maintained in "BMEC medium" composed of Medium 199 (with glucose, Gibco) with added FBS (10%; Invitrogen) and antibiotic/antimycotic (1%). The hAMSCs, GBM cells, and hBMECs were all maintained in an incubator at 37°C and an atmosphere of 5% CO_2.

Retroviral and Lentiviral Production and Infection

To identify hAMSCs in our in vitro coculture and in vivo mouse experiments, we transduced these cells with lentiviral vectors coding for DsRed or green fluorescent protein (GFP)/luciferase proteins [15]. Viral vectors were packaged from HEK293 cells. After collection and concentration, hAMSCs were infected with the viruses and sorted by flow cytometry, as previously described by our group [15].

Conditioned Media, Fibronectin, and Laminin

To collect the soluble factors released by fetal astrocytes and GBM cells, the cells were seeded in standard tissue culture-treated flasks (75 cm^2, BD, Franklin Lakes, NJ, http://www.bd.com) and allowed to grow to near confluence (~80%). The cells were then washed with phosphate-buffered saline (PBS), and the culture medium was changed to serum-free MesenPRO composed of MesenPRO RS basal medium with added antibiotic/antimycotic and GlutaMAX or serum-free BMEC medium, composed of Medium 199 (Gibco) with added antibiotic/antimycotic. The media were then conditioned for 48 hours, collected, and centrifuged to remove cells and debris. This conditioned medium (CM) was stored at −80°C in aliquots and thawed before use. The medium harvested from GBM cells was considered GCM and that harvested from fetal astrocytes was considered noncancerous astrocyte-conditioned medium (NCCM).

Uncleaved fibronectin from human plasma was obtained from Sigma-Aldrich. Soluble fibronectin (120 kDa α-chymotryptic fragment) was obtained from EMD Millipore (Billerica, MA, http://www.emdmillipore.com) and reconstituted according to the vendor's recommendations. LM was obtained from Sigma-Aldrich (as described above) and from BD for use in some experiments, as noted later.

Quantification of Cytokines in Conditioned Media

Conditioned media from U87 GBM and F60 were collected, as described above. The levels of interferon-γ, interleukin (IL)-6, IL-8, tumor necrosis factor-α (TNF-α), monocyte chemotactic protein 1 (MCP-1), and MCP-4 in these conditioned media were then measured using the MesoScale Discovery, V-PLEX multiplex assays, as per the manufacturer's instructions (Sector Imager 2400; Meso Scale Discovery, Gaithersburg, MD, http://www.mesoscale.com).

Pretreatment and Control Conditions of Cells

hAMSCs and hBMECs were pretreated before the experiments according to the following protocols. LM was used to coat the flasks at 2–4 $\mu g/cm^2$, and hAMSCs were grown on these plates for at least 3 passages. In the control case, hAMSCs were grown in standard MesenPRO complete medium. hAMSCs were also exposed to soluble FN diluted in serum-free MesenPRO at 20 $\mu g/ml$ for approximately 6 hours. hAMSCs and BMECs were exposed to 100% GCM, from U87 GBM cells, unless otherwise noted, overnight ($\geq$18 hours), as specified. For the controls, the cells were exposed to serum-free MesenPRO for equivalent portions of time. For the prime preconditioning, the hAMSCs were exposed to LM, GCM, and FN. In these cases, FN was diluted into GCM to achieve simultaneous exposure. In the controls, the cells were cultured in standard medium on LM for 6 hours before the start of the experiment. At that point, the cells were washed with PBS, and the medium was changed to serum-free MesenPRO.

Microfluidic Adherence Assay

The attachment of hAMSCs to monolayers of hBMECs was tested and described in our previous work [21]. In brief, microfluidic chambers were coated with uncleaved FN at 20 $\mu g/ml$ to allow attachment of hBMECs. The hBMECs were allowed to form monolayers overnight inside the device and were subsequently exposed to GCM or serum-free medium (SFM) for an additional 18–24 hours. Subsequently, the hAMSCs were flowed through the chamber at physiologic wall shear stresses of ~0.1 Pa for 4–10 minutes. Before the flow, the hAMSCs were stained with CellTracker Red CMTPX (Invitrogen) to allow visualization of the attached cells during the flow. For each condition, the flow was allowed to continue for an equal period of time before the images were taken. Snapshots were taken during the flow, and the flow rate was sufficient to distinguish mobile cells from stationary cells. High-exposure fluorescent imaging was used to image the mobile cells as dim streaks, and the adhered cells presented as bright spots. The attached cells were counted automatically using MATLAB software (MathWorks, Natick, MA, http://www.mathworks.com).

Transendothelial Invasion Assay

To measure the ability of hAMSCs to breach the monolayers of hBMECs, we followed previously established protocols [22]. In brief, Transwell chambers (model no. 3422; Corning Costar, Acton, MA, http://www.corning.com/lifesciences) with 8-μm pores were first coated with uncleaved FN to allow attachment of hBMECs. The cells were then seeded in these chambers at 4×10^5 cells per milliliter (10^5 cells per insert) and allowed to form monolayers overnight. The next day, the monolayers were washed with PBS, and the hAMSCs were seeded on top of these monolayers at 2×10^5 cells per milliliter (5×10^4 cells per insert) in low-serum MesenPRO, composed of MesenPRO RS basal medium with added antibiotic/antimycotic (1%), GlutaMAX (1%), and 0.5% FBS. The bottom wells of the chambers were filled with 100% conditioned media (F60 or U87 MG) to serve as a chemoattractant. After 24 hours of incubation, the topsides of the inserts were wiped clean, and the bottoms of the inserts were fixed and stained with 4′6-diamidino-2-phenylindole. The hAMSCs used in this experiment were previously engineered to express DsRed to allow distinction from hBMECs. Nine evenly spaced fields were taken from each insert and counted manually by blinded observers to determine the number of transmigrated hAMSCs. Both the absolute number of transmigrated cells and the fold-change in the transmigrated cells were determined.

Nanopattern Cell Migration Assay

The migration speeds of the GBM cells were quantified using a nanopatterned surface, a directional migration assay using nanoridges, and grooves constructed of transparent polyurethane acrylate and fabricated using UV-assisted capillary lithography, as previously reported by our group [23–25]. Before plating the cells, the nanoridged substrata were coated with poly-D-lysine (10 μg/ml) for 15 minutes and mouse laminin (10 μg/ml; BD) for 1 hour. Cell migration was quantified using time-lapse microscopy. Long-term observation was performed with a motorized inverted microscope (Olympus IX81; Olympus, Center Valley, PA, http://www.olympusamerica.com). Phase-contrast and epifluorescent cell images were automatically recorded for 15 hours at 10–20-minute intervals using Slidebook, version 4.1 (Intelligent Imaging Innovations, Denver, CO, http://www.intelligent-imaging.com). The average cell speed, alignment, and persistence were calculated by tracking 75–100 cells per condition using a customized semiautomated MATLAB program (MathWorks) by blinded observers.

Chemotaxis Assays

These assays were designed to measure the cells' speeds in a particular direction, which was toward a gradient of GCM. These experiments were conducted, as previously described [26], using a custom microfluidic device designed to generate gradients across narrow channels. hAMSC motility was restricted to the axis of the narrow, cell-width channels allowing a simple analysis of cell speeds, just as in our migration assay. The gradients were formed in the test case from 0% (SFM) to 100% GCM. In the control case, no gradient was formed before analyzing the cell movements. Motion toward the greater concentration of GCM was considered positive.

An additional assay was also conducted to measure the number of hAMSCs that responded to the GCM gradients. These experiments used uncoated Transwell chambers (model no. 3422; Corning Costar) with 8-μm pores. The hAMSCs were seeded at 1.2×10^5 cells per milliliter (3×10^4 cells per insert) in low-serum MesenPRO, composed of MesenPRO RS basal medium with added antibiotic/antimycotic (1%), GlutaMAX (1%), and 0.5% FBS. The bottom wells of the chambers were filled with 100% GCM (U87 MG) to serve as a chemoattractant. After 18 hours of hAMSC incubation, the topsides of the inserts were wiped clean, and the bottoms of the inserts were fixed and stained using the Diff-Quik staining kit. Nine evenly spaced fields were taken from each insert and counted manually by blinded observers to determine the number of migrated hAMSCs. Both the absolute number of the migrated cells and the fold-change in the migrated cells were determined.

In Vivo Analysis of Homing

The Johns Hopkins School of Medicine Animal Care and Use Committee approved all the animal protocols. For intracranial tumor xenografts, severe combined immunodeficiency mice were stereotactically injected with 7×10^5 viable U87 MG cells in 3 μl of DMEM/F12 serum media without growth factors intracranially into the right striatum. The cells were allowed to form tumors for 3 weeks before injections of the MSCs were performed. Cell viability was determined using trypan blue dye exclusion.

The hAMSCs engineered to express GFP/luciferase were grown under control conditions or exposed to prime pretreatment before the experiment. Three weeks after tumor inoculation, 4×10^5 hAMSCs were systemically injected either into the left cardiac ventricle or tail vein, as previously described [15, 27]. After 2 weeks, the mice were perfused and the brains were extracted and cryosectioned. The decision to measure engraftment of the hAMSCs to the tumor at the 2-week time point was made according to previous protocols and studies by our group that showed that when injected into mice-bearing human GBM, luciferase-labeled hAMSCs were detectable for up to 2 weeks by bioluminescence but afterward experienced a significant decline in bioluminescent signal and were virtually undetectable in vivo [15]. These studies also showed the absence of hAMSCs or tumor-associated fibroblasts at 60 days after injection. Hematoxylin and eosin staining was first used to identify the tumor borders across the length of the brain. Sections from the tumor region were then immunostained for GFP and human nuclei. The cells were counted automatically using a custom MATLAB program designed to segment and identify fluorescent signals. The hAMSC numbers were counted and normalized relative to the total number of human nuclei at the tumor site.

Differentiation and Proliferation Assays

Differentiation assays were performed to determine the differentiation capacities of hAMSCs, as previously described [18, 15]. In brief, the cells were seeded into 24-well plates (42,000 cells per well for adipogenic differentiation, 8,400 cells per well for osteogenic differentiation) or cultured as pellets (2.5×10^5 cells per tube for chondrogenic differentiation). For the positive controls, the cells were then exposed to differentiation conditions using adipogenic, osteogenic, or chondrogenic supplements (CCM007-008 and CCM011; R&D Systems, Minneapolis, MN, http://www.rndsystems.com). For the negative controls, MesenPRO complete media without differentiation supplements were used. The cell lineage was evaluated using Oil Red O for adipocytes (00625; Sigma-Aldrich), Alizarin Red S for osteocytes (AB5533; Sigma-Aldrich), and Masson's trichrome staining for chondrocytes.

An MTT assay (CellTiter 96 AQueous One Solution Proliferation Assay; Promega, Madison, WI, http://www.promega.com) was performed to evaluate the effect of conditioning on cell proliferation [15]. hAMSCs or U87 tumor cells (1,000 cells per well) were seeded in 96-well plates and cultured in control or prime media. Cell proliferation was analyzed every 3 days in triplicate for each experimental condition.

Statistical Analysis

The results are presented as the mean $\pm$ SEM. The Mann-Whitney rank sum test was used for pairwise comparisons, and Dunn's test (rank-based analysis of variance [ANOVA]) was used for the multiple group comparisons. In some cases, as noted, Student's *t* test or the standard ANOVA, Holm-Sadik method was used. Where indicated, 2-way ANOVA was used for a comparison of multiple, simultaneously present factors. The statistics were analyzed using SigmaPlot (Systat Software, Inc., San Jose, CA, http://www.systat.com) and GraphPad Prism, version 5, software (GraphPad, San Diego, CA, http://www.graphpad.com). For precision, all experiments were repeated to ensure reproducibility; $p < .05$ was considered statistically significant.

RESULTS

Firm Adhesion to Brain Endothelium

The initial portions of the homing process involve interactions between hAMSCs and the vascular endothelium, whereby hAMSCs must adhere to the vessel wall (steps 1–3; Fig. 1A). This process was modeled using a microfluidic flow chamber, consisting of a molded silicon rubber chip bonded to tissue culture glass (Fig. 2A, 2B). This chamber was coated with a monolayer of hBMECs to mimic the luminal surface of a blood vessel (Fig. 2C). Because fluorescently tagged hAMSCs flowed over the hBMEC monolayer, the numbers of attached stem cells were quantified over defined time periods (Fig. 2D; supplemental online Video 1).

It is well known that inflammation induces expression of cell-adhesion receptors in endothelial cells [3, 16]. GBM cells are known to secrete certain signaling molecules that have been implicated in inflammation and homing, such as MCP-1 [28] and interleukin-6 [29, 30]. Thus, to simulate the inflamed tumor microenvironment, we exposed hBMEC monolayers to GCM overnight ($\geq$18 hours). We observed significantly increased adherence of hAMSCs to GCM-treated monolayers (sample 549-generated GCM in this case) compared with those exposed to SFM (1.6-fold increase, $p < .05$; Fig. 2E; supplemental online Fig. 1A). Thus, the monolayers were exposed to GCM in all subsequent experiments to model inflamed endothelium.

Next, we examined whether preconditioning of hAMSCs would increase adherence of these cells to vascular endothelium. We observed that exposure of hAMSCs to GCM overnight also significantly increased their adherence (2.5-fold increase, $p < .05$; Fig. 2F; supplemental online Fig. 1B). The adherence was mediated in part by the specific protein, VLA-4. This integrin complex ($\alpha 4\beta 1$) mediates firm adhesion, because it binds cell surface molecules expressed by vascular endothelial cells [3, 21]. To target this adhesion mediator, we pre-exposed hAMSCs to FN, a known ligand of VLA-4. We found that the cells treated with FN for 6 hours before the start of the experiment showed greater adherence to hBMEC monolayers (2.1-fold increase, $p < .05$; Fig. 2G; supplemental online Fig. 1C). These results indicated that pre-exposing hAMSCs to GCM and FN can increase endothelial docking of hAMSCs to endothelium in the vicinity of glioblastoma tumors.

Transmigration Through the Blood-Brain Barrier

The next critical step of homing in the brain is transmigration through vascular endothelium (i.e., breaching the BBB; step 4, Fig. 1A). Using previously established protocols [22, 31], the BBB was modeled by growing monolayers of hBMECs on the top surfaces of membranes in 8-μm-pore Transwell chambers (Fig. 3A). Subsequently, the hAMSCs were incubated on top of this monolayer, and the number of cells that crossed the monolayer and membrane were counted. We focused on cell movement through the endothelial cell monolayers; thus, we used the 8-μm large-pore membranes to avoid major obstruction once the monolayer had been breached. Conditioned media (either GCM or NCCM) were presented in the bottom well of the Transwell chambers to activate the hBMEC monolayer and to serve as a chemoattractant for the hAMSCs (Fig. 3A). Compared with the control SFM, only GCM induced significant movement of the hAMSCs through the endothelial monolayers (5.8-fold increase, $p < .05$; Fig. 3B; supplemental online Fig. 2A). Because no significant differences were observed between SFM and NCCM ($p > .05$), subsequent experiments used SFM as a negative control.

We then examined whether preconditioning of hAMSCs could enhance transmigration. In these experiments, we observed the movement of cells toward SFM and GCM as chemoattractants, reporting the normalized ratio. In this manner, our results display the selectivity of cell movement toward gliomas. The process of transmigration is heavily dependent on the physical interactions between the invading stem cells and the vascular endothelium [16, 31]. Therefore we again used GCM and FN pretreatment to enhance the ability of hAMSCs to breach the BBB. We observed significant increases in selectivity after both GCM preconditioning (GCM vs. control, 22.9 vs. 11.9, $p < .05$; Fig. 3C; supplemental online Fig. 2B) and FN preconditioning (FN vs. control, 63.7 vs. 9.5, $p < .05$; Fig. 3D; supplemental online Fig. 2C). Moreover, hAMSCs were also exposed to immobilized FN (immobilized FN vs. control, 13.8 vs. 7.7, $p < .05$; supplemental online Fig. 3A). Immobilized FN enhanced transmigration toward GCM, just as seen with soluble FN (supplemental online Fig. 3B). Our findings suggest that pretreatment with GCM and FN can better prepare hAMSCs to breach the BBB near tumor sites.

Migration Along ECM Structures

Additional experiments modeled the movement of hAMSCs through the brain parenchyma toward the tumor (step 5, Fig. 1A). We first focused on the nondirectional motility of cells to analyze their general migratory status. To model the ECM structures commonly encountered in the brain (e.g., myelinated fiber tracts and vasculature), we used nanometer scale-patterned surfaces consisting of parallel ridges. Similar to our previous studies [15, 23], we coated these engineered surfaces with the ECM protein LM to facilitate cell attachment and mimic more closely the brain tissue microenvironment. We then monitored and quantified the movements of the hAMSCs via time-lapse microscopy as they elongated and migrated parallel to the patterned ridges (Fig. 4A; supplemental online Video 2) and quantified the migration using three single cell metrics: speed, alignment, and persistence. Alignment of cell movement was measured by calculating the ratio of distances traveled parallel versus perpendicular to the ridge pattern, a measure shown to correlate with the strength of the interactions between the cells and the underlying substratum [24]. Persistence was calculated as the ratio of the final distance from the start to the end of a cell trajectory versus the total trajectory length. The value of this metric specifies the degree to which a trajectory is similar to a straight line traveled in one direction versus random, undefined exploration.

This part of the analysis was designed to simulate hAMSC migration in the vicinity of a brain tumor. Therefore, first we explored the effect of cell exposure to GCM during the entire experiment, resulting in enhanced migration compared with cells exposed to SFM (GCM vs. SFM: speed, 14.6 vs. 12.7, $p < .05$; alignment, 1.9 vs. 1.7, $p < .05$; persistence, 0.2 vs. 0.1, $p < .05$, Fig. 4B). During subsequent experiments, the cells were observed migrating in the presence of GCM to model the tumor microenvironment.

Next, we pretreated hAMSCs in several ways to enhance their motility. Pre-exposure of hAMSCs to GCM overnight resulted in significant increases in migration speed and alignment (GCM vs. control: speed, 21.6 vs. 17.9, $p < .05$; alignment, 3.6 vs. 2.6, $p < .05$, Fig. 4C). Moreover, long-term pre-exposure of hAMSCs

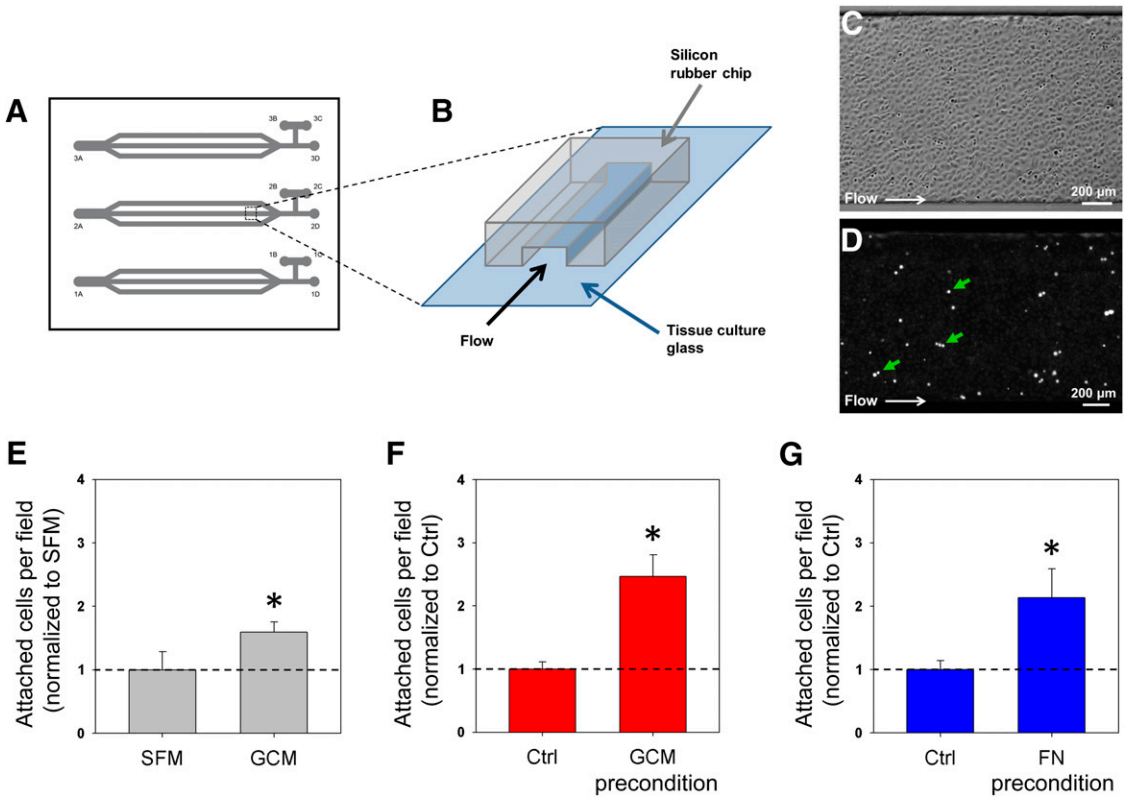

Figure 2. Pretreatment of mesenchymal stem cells (MSCs) enhanced brain endothelium attachment. **(A, B):** Schematic of single-layer microfluidic flow chamber device used to model a blood vessel. **(C):** Phase contrast image showing a monolayer of human brain microvascular endothelial cells (hBMECs) in the flow chamber. **(D):** Fluorescent image of the same field. Fluorescently stained human adipocyte-derived MSCs (hAMSCs) (green arrows) have firmly attached to the hBMEC monolayer during the flow experiment. Stained, rounded hAMSCs were visualized and quantified using computer software. **(E–G):** Quantification of hAMSC attachment to monolayers under various conditions. Values are normalized and expressed as the fold change (mean ± SEM, ∗, $p < .05$, Mann-Whitney rank sum test). **(E):** Monolayers were exposed to SFM or sample 549 GCM to simulate inflammation ($n = 15$ fields). Monolayers were exposed to GCM in all subsequent experiments **(F, G)**. hAMSCs were pre-exposed to GCM overnight (**F**, $n \geq 13$ fields) or soluble FN for 6 hours (**G**, $n \geq 13$ fields). In control conditions, hAMSCs were exposed to SFM for equivalent portions of time (overnight or 6 hours). Abbreviations: Ctrl, control; FN, fibronectin; GCM, glioma-conditioned medium; SFM, serum-free medium.

to LM, which is highly expressed in vascular and perivascular regions of the brain [32–34], significantly enhanced the migration speed compared with cells cultured under control conditions (LM vs. control: speed, 18.1 vs. 15.6, $p < .05$, Fig. 4D). In these experiments, the cells were grown on LM for at least three passages before harvesting. The enhanced migratory effects after GCM preconditioning were also seen using a primary hAMSC sample (GCM vs. SFM: speed, 13.1 vs. 5.0, $p < .05$; alignment, 3.9 vs. 3.1, $p < .05$; persistence, 0.4 vs. 0.2, $p < .05$; supplemental online Fig. 4A, 4B). The increases in migration speed induced by growth on LM were also present when the cells were observed migrating under different media conditions (e.g., control medium with and without serum; serum: LM vs. control, 48.3 vs. 38.6, $p < .05$; SFM: LM vs. control, 16.0 vs. 13.6, $p < .05$; supplemental online Fig. 4C). These results have indicated that environmental cues, namely those presented by gliomas, can enhance hAMSC motility in an in vitro model that closely recapitulates their natural environment.

Chemotaxis Toward Glioma

The final set of in vitro studies focused on stem cell chemotaxis toward glioma (step 5, Fig. 1A). We used two separate models to analyze chemotaxis. First, we developed a microfluidic device capable of generating linear gradients of solubilized factors (Fig. 5A) [26]. In this device, the cells are restricted to narrow, cell-width channels that bias cell movements parallel to the axis of the gradient, thus facilitating the analysis of the chemotactic gradient-induced bias in cell migration directionality. To simulate the release of protein signals from a tumor, gradients of GCM ranging from 0% (SFM) to 100% (neat) were established. The cell movements were observed via time-lapse microscopy, and migration was quantified based on the rate of motion toward the greater GCM concentration (supplemental online Video 3). We observed a clear difference in speed and persistence of hAMSC movements toward greater GCM concentrations compared with the negative control, SFM (no gradient, 0%–0%; GCM vs. SFM, speed 0.21 vs. −0.03, $p < .05$; persistence, 2.3 vs. −0.1, $p < .05$, Fig. 5B). No enhancements were observed in the speeds or persistence toward GCM after pretreatment of hAMSCs with GCM (data not shown). We restricted our pretreatment methods to those directly related to the stimuli present in each experimental model, reasoning that these perturbations were more likely to produce the desired effects. Furthermore, because our chemotaxis studies focused on the cellular responses to GCM, we initially investigated only pretreatment using GCM.

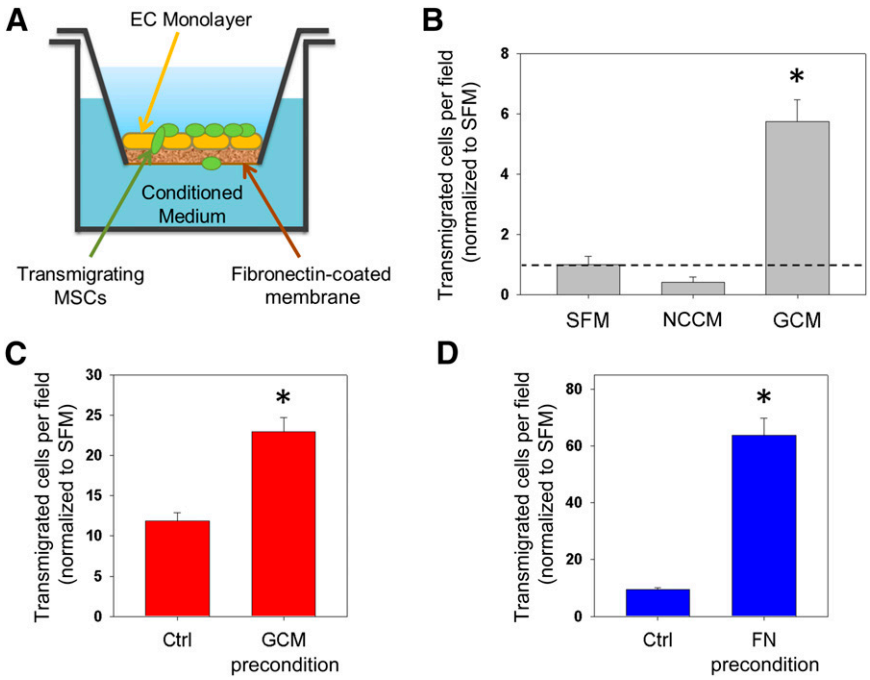

Figure 3. Pretreatment of MSCs enhances transmigration through the blood-brain barrier (BBB). **(A):** Schematic of 8-μm-pore Transwell chamber coated with human brain microvascular endothelial cells (hBMECs) monolayer to simulate the BBB. **(B–D):** Quantification of human adipose-derived MSC (hAMSCs) transmigration through hBMEC monolayers under various conditions. Values are normalized and expressed as the fold change ($n = 27$ fields, mean $\pm$ SEM, $*$, $p < .05$, Mann-Whitney rank sum test). **(B):** SFM, NCCM, or GCM served as chemoattractants/activators of monolayers. **(B–D):** hAMSCs were subjected to overnight GCM pretreatment **(C)** or 6-hour FN pretreatment **(D)**. In control conditions, hAMSCs were exposed to SFM for equivalent portions of time (overnight or 6 hours). Abbreviations: Ctrl, control; EC, endothelial cell; FN, fibronectin; GCM, glioma-conditioned medium; MSC, mesenchymal stem cell; NCCM, noncancerous astrocyte-conditioned medium.

Our second chemotaxis model used standard 8-μm-pore Transwell chambers, with uncoated membranes (Fig. 5C). Conditioned media were loaded in the bottom wells to serve as chemoattractants and form gradients across the membranes. With no proteins or cells coating the membrane or restricting motion, this platform could measure the numbers of cells that responded to the gradient by crossing the membrane. Just as with our transmigration study, only GCM could induce significant increases in cell movements across the membrane (GCM vs. SFM vs. NCCM, 3.8 vs. 1.0 vs. 0.9, $p < .05$ for GCM vs. other media; Fig. 5D; supplemental online Fig. 5A). Pretreatment of hAMSCs with GCM induced significant increases in the numbers of cells responding to the gradient (GCM vs. control, 1.6-fold increase, $p < .05$; Fig. 5E; supplemental online Fig. 5B). These experiments indicated that pretreatment of hAMSCs can increase the number of responsive cells, possibly by enhancing their sensitivity to GCM. However, pretreatment might not increase the rate at which the cells approach the source of the soluble signals in GCM (i.e., the brain tumor).

With these results, we have demonstrated in two ways (Figs. 3B, 5D) that only GCM can induce significant cell movements across Transwell membranes. We attempted to identify potential unique soluble factors released by glioma but not by astrocytes that could be responsible for the preferred movement of hAMSCs toward GCM as a chemoattractant. Using sandwich immunoassays to analyze the protein concentrations, we found that levels of the human-secreted proinflammatory markers interferon-γ ($p < .05$), IL-6 ($p < .0001$), IL-8 ($p < .0001$), and TNF-α ($p < .0001$) were significantly greater in gliomas-conditioned media compared with astrocyte-conditioned media (Fig. 6A–D). In contrast, the levels of human secreted chemokines, MCP-1 ($p < .0001$) and MCP-4 ($p < .0001$), were significantly greater in astrocyte-conditioned media compared with GCM (Fig. 6E, 6F). Although individual proinflammatory cytokines implicated in stem cell migration (IFN-γ, IL-6, IL-8, TNF-α) were expressed at greater levels in GCM as expected, the chemokines MCP-1 and MCP-4 were expressed at much higher levels in NCCM, an unexpected finding. This might have been because the source of the NCCM was fetal astrocytes, which are still in a developmental stage in which chemokines and morphogens are normally expressed as a part of neurodevelopment.

Pretreatment With Numerous Simultaneously Presented Stimuli

Throughout these experiments, we have demonstrated that different preconditioning techniques can enhance several steps of the homing process in vitro. Next, we sought to determine whether the corresponding environmental cues can work in concert to mediate enhancements of these steps simultaneously. Our subsequent investigations thus involved a combination of all three environmental perturbations, which we termed “prime” (GCM plus FN plus LM; Fig. 1C). We began these studies with observations of firm adhesion to brain endothelium (Fig. 2). Prime preconditioning of hAMSCs induced a significant, 2.2-fold, increase in attachment to hBMEC monolayers ($p < .05$; Fig. 7A; supplemental online Fig. 6A). We used this same prime preconditioning approach to induce similar enhancements in transmigration, migration, and chemotaxis (prime vs. control:

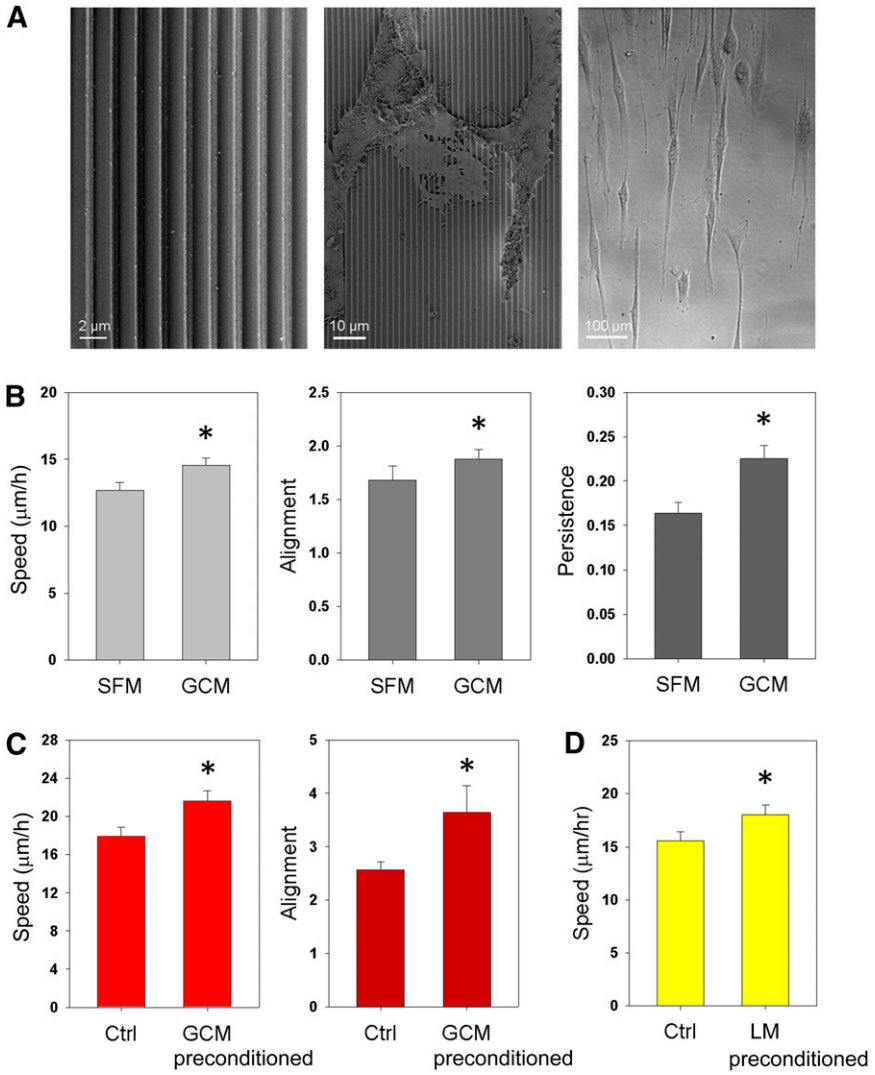

Figure 4. Pretreatment of mesenchymal stem cells (MSCs) enhances migration along extracellular matrix structures. **(A):** Left: Scanning electron micrographic image of topographic pattern with parallel ridges 350 nm wide, 350 nm deep, spaced 1.5 μm apart. Middle: Scanning electron microscope images of human adipocyte-derived MSCs (hAMSCs) cultured on ridge pattern for 24 hours in vitro. Right: Phase contrast image of hAMSCs elongating and migrating on ridge pattern. **(B):** Quantification of hAMSC migration measured by speed, alignment, and persistence. The cells were exposed to SFM or GCM during the entire experiment ($n \geq 75$ cells, mean $\pm$ SEM, $*$, $p < .05$, Mann-Whitney rank sum test). **(C, D):** Quantification of hAMSC migration measured by speed and alignment, following preconditioning ($n \geq 75$ cells, mean $\pm$ SEM, $*$, $p < .05$, Mann-Whitney rank sum test). The cells were pre-exposed to GCM or SFM (Ctrl condition) overnight before the experiment. Subsequently, all cells were exposed to GCM during the experiment **(C)**. The cells were grown on LM or on standard, uncoated tissue culture surfaces (Ctrl condition) for 3 weeks before the experiment. All cells were exposed to GCM during the experiment **(D)**. Abbreviations: GCM, glioma-conditioned medium; LM, laminin; SFM, serum-free medium.

transmigration, 84.8 vs. 27.6, $p < .05$; Fig. 7B; supplemental online Fig. 6B; migration speed, 20.2 vs. 14.7, $p < .05$; Fig. 7C; migration alignment, 2.6 vs. 1.8, $p < .05$; Fig. 7C; chemotaxis, 2.0 vs. 1.0, $p < .05$; Fig. 7D; supplemental online Fig. 6C). These findings have demonstrated that the individual improvements induced by each perturbation are conserved when the techniques are combined. These experiments have shown that priming the cells results in increased adhesion, transmigration, migration, and chemotaxis.

Effects of Pretreatment on MSC Proliferation and Differentiation

Obvious concerns exist regarding the effects that the pretreatment might have on MSCs. To address these issues, we observed the proliferation, differentiation, and cell surface marker expression of the hAMSCs after prime (GCM plus FN plus LM) pretreatment. Preconditioned cells demonstrated nearly identical expression of commonly accepted MSC markers, including CD31, CD34, CD45, CD73, CD90, CD105 (supplemental online Fig. 7), and maintained the ability to differentiate into multiple lineages, including adipocytes, osteocytes, and chondrocytes (supplemental online Fig. 8). Moreover, prime pretreatment did not increase the growth rate of hAMSCs (supplemental online Fig. 9A) and also did not alter their effects on GBM cell growth (supplemental online Fig. 9B). Together these findings have shown that modest culturing methods can improve the ability of MSCs to localize to tumors, without altering the identity or behaviors of the cells.

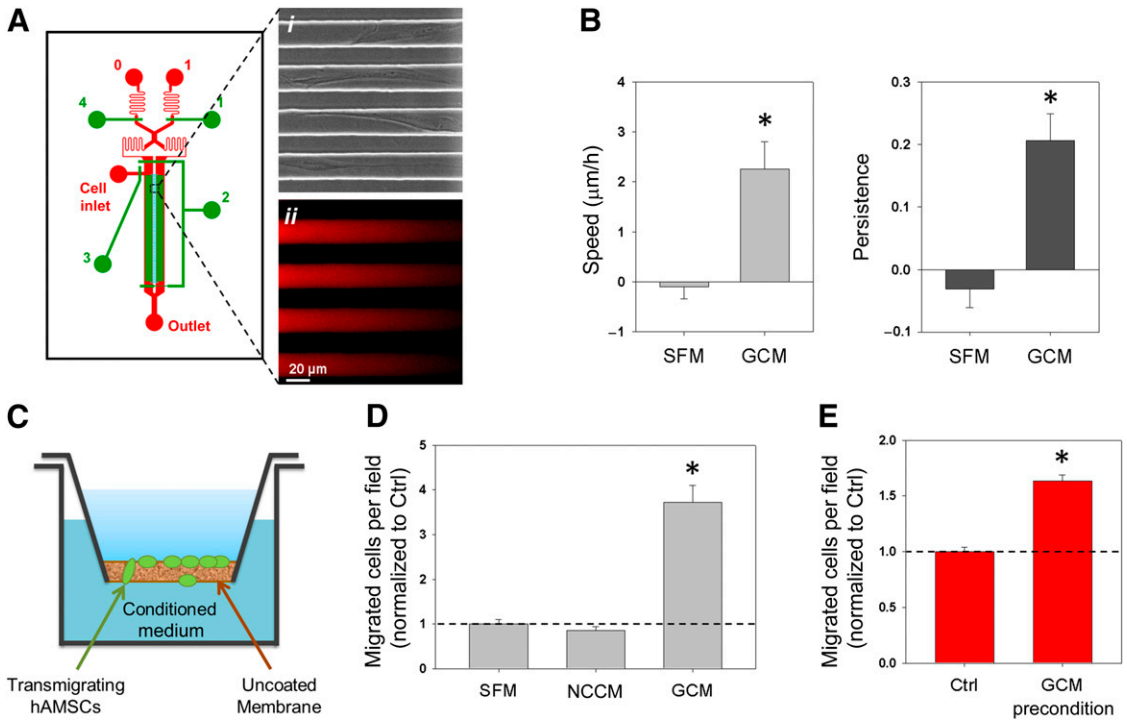

Figure 5. Pretreatment of mesenchymal stem cells enhances chemotaxis toward gradients of GCM. **(A):** Schematic of multilayer microfluidic device used to generate gradients of GCM. The red layer represents the cell loading areas. Light blue highlights the narrow channels where linear gradients form. Green represents control layers used to operate the device. **(Ai):** Phase contrast image of hAMSCs moving through narrow channels. **(Aii):** Channels filled with Alexa Fluor 594 fluorescent dye, allowing visualization of gradients in the device. **(B):** Quantification of hAMSC chemotaxis measured by speed and persistence. Cells migrated toward 100% GCM or the negative control, SFM. Movement toward the higher concentration was considered positive ($n \geq 60$ cells, mean $\pm$ SEM, $*$, $p < .05$, Mann-Whitney rank sum test). **(C):** Schematic of 8-μm-pore Transwell chamber used to analyze sensitivity to gradient. **(D, E):** Quantification of hAMSC chemotaxis measured by numbers of cells migrating through the membrane. Values are normalized and expressed as the fold change ($n = 27$ fields, mean $\pm$ SEM, $*$, $p < .05$, Mann-Whitney rank sum test). **(D):** SFM, NCCM, or GCM served as the chemoattractant. **(E):** hAMSCs were subjected to overnight GCM pretreatment. In the Ctrl condition, hAMSCs were exposed to SFM overnight. Abbreviations: Ctrl, control; GCM, glioma-conditioned medium; hAMSC, human adipocyte-derived mesenchymal stem cell; NCCM, noncancerous astrocyte-conditioned medium; SFM, serum-free medium.

In Vivo Validation of Homing Enhancements

Having demonstrated that environmental perturbation of hAMSCs can enhance several putative homing steps in vitro, we next sought validation of these results using an orthotopic animal model of human GBM. Thus, 7×10^5 U87 GBM cells were stereotactically injected into the right striatum of athymic nude mice, as previously described [15, 23, 35]. To analyze the homing capacities in vivo, we injected hAMSCs engineered to express GFP systemically, 3 weeks after tumor cell injection. We delivered 4×10^5 hAMSCs via systemic injections (Fig. 7E). An estimate of the amount of injected cells that reached the tumor was generated by quantifying the number of hAMSCs per slice. Approximately 0.1% of hAMSCs injected intracardiac manner reached the tumor but fewer than one half of this amount reached the tumor from the tail injections, consistent with the low efficiency of MSC localization to brain injuries observed in previous studies (<1% engraftment). However, 2 weeks after injection, we observed significantly greater tumor engraftment of GFP-hAMSCs cultured under prime conditions compared with control hAMSCs (prime vs. control: 6.67 vs. 1.0, $p < .05$, Fig. 7F–G).

Greater numbers of hAMSCs were observed colocalized to tumors from intracardiac injections than from intravenous injections (supplemental online Fig. 6D). However, for both delivery methods, prime pretreatment resulted in a similar fold-increase (>6) in colocalization. Owing to the significant variability in tumor sizes across the mice, colocalization was quantified as the percentage of hAMSCs per total human nuclei in a given brain slice.

An additional concern from our in vivo colocalization study arose from the safety of the injection methods; 3 of 5 mice receiving intracardiac injections of control hAMSCs had died immediately after the procedure, resulting in a reduced number of mice in the control condition. In a follow-up study, we injected mice with a reduced number of hAMSCs (2×10^5) to reduce the risk of occlusion.

Moreover, when using intracardiac injections of a smaller number of hAMSCs, fluorescently tagged hAMSCs were observed at the site of the tumor only in the mice receiving the prime pretreated hAMSCs compared with the control (supplemental online Fig. 10). In the present study, we also examined the brain regions outside the tumor for hAMSC engraftment. Imaging for fluorescently tagged hAMSCs outside of the tumor region showed no significant amount of hAMSC localization to areas outside the tumor. In a few cases, the cells were observed nearby, but directly outside, the tumor. No significant differences were found between the pretreatment conditions with respect to hAMSC homing to brain regions outside the tumor (data not shown). These in vivo findings support the homing enhancements we observed in vitro

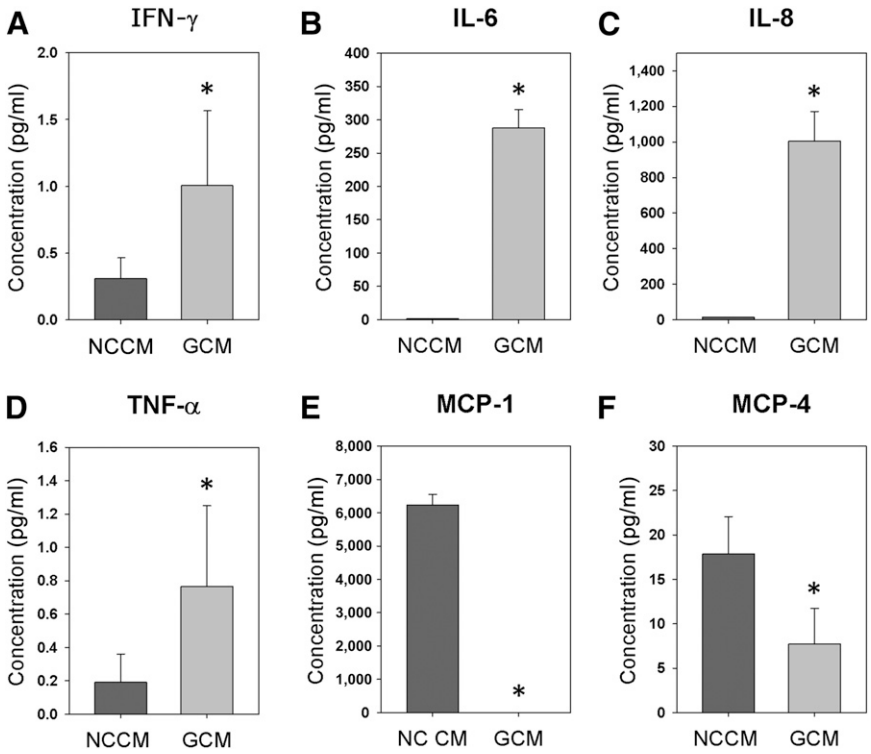

Figure 6. GCM contains higher levels of secreted proinflammatory markers implicated in mesenchymal stem cell migration compared with NCCM. Levels of IFN-γ, IL-6, IL-8, TNF-α, MCP-1, and MCP-4 in both GCM and NCCM were measured by MesoScale Discovery (MSD) multiplex assays as per manufacturer's instructions. Values are expressed as the concentration (mean $\pm$ SEM, Mann-Whitney rank sum test). Levels of IFN-γ ($p < .05$) **(A)**, IL-6 ($p < .0001$) **(B)**, and IL-8 ($p < .0001$) **(C)** were significantly higher in GCM than in NCCM. Levels of TNF-α ($p < .05$) **(D)**, MCP-1 ($p < .0001$) **(E)**, and MCP-4 ($p < .01$) **(F)** were significantly higher in NCCM than in GCM. Abbreviations: GCM, gliomas-conditioned medium; IFN-γ, interferon-γ, IL, interleukin; MCP, monocyte chemotactic protein; NCCM, noncancerous astrocyte-conditioned medium; SFM, serum-free medium; TNF-α, tumor necrosis factor-α.

and further demonstrate that environmental perturbations of hAMSCs ("prime" preconditioning with GCM plus FN plus LM) can enhance homing to gliomas.

Discussion

Substantial clinical potential exists for novel stem cell-based therapies for neurological disorders, including strokes, neurodegenerative diseases such as Parkinson's, and brain tumors. Specifically, MSCs are thought to have the greatest therapeutic potential via their trophic, paracrine, and immunomodulatory functions. They can modulate the regenerative environment by secreting anti-inflammatory molecules such as IL-1, IL-2, IL-12, TNF-α, and IFN-γ and immunomodulate via a wide variety of secreted proteins, including prostaglandin-2, transforming growth factor-β1, hepatocyte growth factor, stromal-derived factor-1, nitric oxide, indoleamine-2,3-dioxygenase, IL-4, IL-6, IL-10, IL-1 receptor antagonist, and soluble TNF-α receptors. They can exist as perivascular pericytes, which extend their cellular processes within blood vessel lumens and monitor the systemic signals within their environment to respond to injury, infection, and other disease processes. This accounts for their ability to mobilize to sites of injury in all vascularized tissues of the body, including the brain. However, the process of getting stem cells safely and efficiently to their target destination for therapeutic purposes has been poorly explored. Recent investigations of stem cell-based treatments of brain disorders have often relied on direct injections into the brain parenchyma [13, 14, 36–39] to avoid concerns of the homing abilities [13, 14, 22, 23, 40, 41]. These invasive approaches can be used after brain surgery for cancer but are challenging in many other cases of neurological disorders because of the iatrogenic risks and inherent difficulty with repeated injections. In order to make systemic stem cell therapies a reality, stem cell homing and engraftment must achieve greater efficiency [3, 13, 14]. The present investigation aimed to enhance stem cell homing through a simple, comprehensive, cell preconditioning-based approach that has important experimental, translational, and clinical implications.

In our report, we have demonstrated that pre-exposure to soluble factors released by glioma increases the homing of MSCs toward glioblastoma in vivo. However, the rationale for developing optimized homing of MSCs is based on the assumption that increases homing might increase the efficacy of MSCs against brain cancer. The real potential of MSCs as a brain cancer therapeutic lies in their use as vehicles for the delivery of anti-cancer proteins such as bone morphogenic protein 4 (BMP-4) [42]. We have shown in a previous study that hAMSCs modified to secrete BMP-4 increased survival in a murine model of human GBM, despite having decreased migration speed and tropism toward the tumor [15]. Developing new methods to augment MSC tropism toward brain cancer might improve therapeutic MSC delivery specifically to the tumor site and improve the efficacy.

We have successfully examined various facets of the homing process through the implementation of several in vitro models

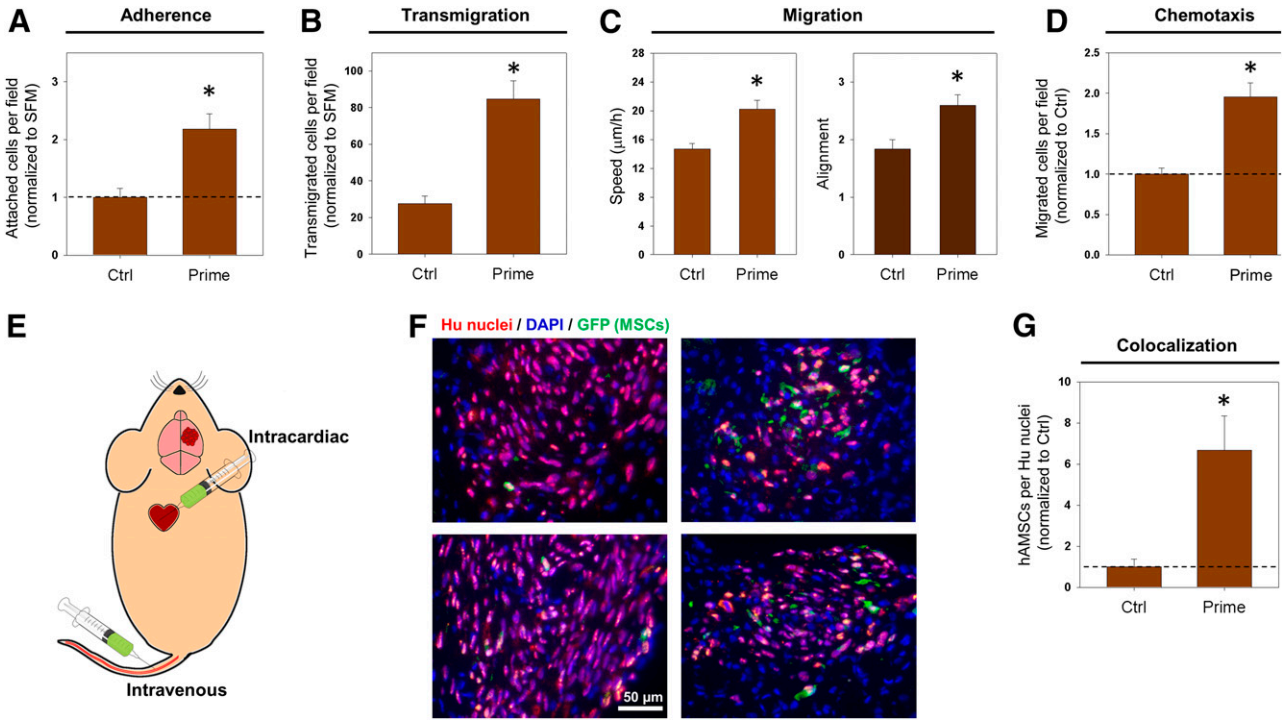

Figure 7. Priming MSCs enhances in vivo brain tumor homing. hAMSCs were pre-exposed to GCM overnight, fibronectin for 6 hours, and laminin for 3 weeks in a single protocol denoted "prime." In Ctrl conditions, hAMSCs were grown on standard, uncoated tissue culture surfaces for 3 weeks and exposed to SFM overnight, before the experiments. **(A):** Quantification of hAMSC attachment to monolayers using microfluidic flow chamber device (shown in Fig. 2). Values are normalized and expressed as the fold change ($n \geq 40$ fields, mean $\pm$ SEM, $*$, $p < .05$, Mann-Whitney rank sum test). **(B):** Quantification of hAMSC transmigration through human brain microvascular endothelial cell monolayers using the protocol described in Figure 3. The values are normalized and expressed as the fold change ($n = 27$ fields, mean $\pm$ SEM, $*$, $p < .05$, Mann-Whitney rank sum test). **(C):** Migration of hAMSCs on nanometer scale-patterned surface as described in Figure 4. Quantification of hAMSC migration measured by speed and alignment ($n \geq 74$ cells, mean $\pm$ SEM, $*$, $p < .05$, Mann-Whitney rank sum test). **(D):** Quantification of hAMSC chemotaxis measured by numbers of cells migrating through membrane. Values are normalized and expressed as fold change ($n = 27$ fields, mean $\pm$ SEM, $*$, $p < .05$, Mann-Whitney rank sum test). **(E):** Schematic depicting methods of injection of 4×10^5 GFP-tagged hAMSCs after tumor formation in mouse models. **(F):** Epifluorescent images of mouse brain cryosections after intracardiac injection of control (left) or prime (right) pretreated hAMSCs. Mouse brain cryosections were stained for human nuclei (red) to identify all injected cells (glioblastoma and hAMSCs). Staining for GFP was used to identify fluorescently tagged hAMSCs. **(G):** Quantification of numbers of hAMSCs observed colocalized with tumors formed by U87 glioblastoma cells. Values are normalized and expressed as the fold change (control: 6 mice [4 tail, 2 heart]; prime: 6 mice [3 tail, 3 heart]; mean $\pm$ SEM, $*$, $p < .05$, Mann-Whitney rank sum test). Abbreviations: Ctrl, control; DAPI, 4′,6-diamidino-2-phenylindole; GCM, glioma-conditioned medium; GFP, green fluorescent protein; Hu, human; hAMSC, human adipose-derived mesenchymal stem cell; MSCs, mesenchymal stem cells; SFM, serum-free medium.

designed to closely resemble in vivo conditions. Advances in micro- and nanotechnology have enabled us to carefully model cell-cell and cell-matrix interactions and the chemical composition of the cell microenvironment. Thus, we were able to screen various perturbations to hAMSCs to develop an optimized preconditioning protocol that could be validated through subsequent in vivo trials. A significantly greater absolute number of hAMSCs were observed colocalized to tumors via intracardiac injections compared with intravenous injections, at the cost of increased mortality. However, both injection methods experienced a greater than sixfold increase in hAMSC colocalization with the optimized preconditioning protocol. This might have resulted from the successive enhancement of multiple homing steps, independent of the administration route. In future studies, the effect of different administration routes on hAMSC homing to tumors could be investigated.

Classic studies have typically used genetic modification of a single protein implicated in homing [21, 40, 41, 43, 44]. However, the adaptive stem cell responses leading to enhanced homing might involve more complex changes in the genotypic and phenotypic repertoire. The current understanding of the pathways governing homing responses is somewhat fragmentary and could remain so for some time. Therefore, inducing adaptive responses of stem cells before their use might be a more direct and effective method to induce the desired changes in their behavior, even in such a complex and multifaceted process as homing. In addition, cell conditioning-based homing enhancement might prove easier to implement for autologous cell therapies, obviating the need for genetic manipulation.

Our analysis represents a first step in the guided, preconditioning-based enhancement of stem cell targeting toward brain tumors. However, additional work is needed to optimize the stem cell delivery to tumor sites and their local therapeutic efficacy. First, our findings were limited to trafficking of nonengineered hAMSCs. Future work could combine the cell culture-based homing enhancements, with the therapeutic effects of an engineered, secreted proteins to enhance therapeutic effects such as TNF-related apoptosis-inducing ligand [14, 36, 39, 45], IL-12 [9], and BMP-4 [15, 42] on hAMSCs for glioma therapy. Second, we chose to use hAMSCs instead of other types of

stem cells, including neural and bone marrow-derived stem cells, because hAMSCs are considered easier to obtain, more genetically and morphologically stable in long-term culture, have a lower senescence ratio, and have a greater proliferative capacity than other stem cell types. Therefore, the findings of the present study might not be applicable to other stem cell types [15, 18]. Moreover, our work focused on brain cancer targeting, and future studies should evaluate whether these findings are also applicable to other neurological pathologies, including stroke, demyelinating diseases such as multiple sclerosis, and neurodegenerative conditions, such as Parkinson's disease. With these caveats in mind, our results present strong evidence that for many pathologies, including those not necessarily located in the brain, mimicking local environmental conditions as a method to precondition stem cells could be very effective to enhance their migration to areas of injury in a site-specific manner.

Conclusion

Systemic stem cell therapy of neurological disorders is currently limited because of the inefficiency of stem cell homing to pathologies within the central nervous system. By simulating the events that occur during stem cell trafficking, we have demonstrated that preconditioning or "priming" hAMSCs with GCM, FN, and LM can simultaneously increase the effectiveness of the multiple steps required for stem cell homing toward GBM. Moreover, using an in vivo animal model of human GBM further supported the effectiveness of these preconditioning techniques. These methods could also prove useful for other neurological disorders, including stroke, demyelinating diseases such as multiple sclerosis, and neurodegenerative diseases such as Parkinson's.

Acknowledgments

We thank the Department of Neurological Surgery and Oncology at Johns Hopkins Hospital for access to intraoperatively obtained glioblastoma and adipose tissues; Candice Shaifer, Lakesha Johnson, Kristy Yuan, and Liron Noiman for establishing the primary cell cultures of glioblastoma and adipose tissue specimens; Deok-Ho Kim for early assistance in the design of the nanopatterned devices; the Piotr Walczak Laboratory at Johns Hopkins University School of Medicine for the kind gift of human microvascular endothelial cells; the P. Charles Lin Laboratory at the National Cancer Institute (Frederick, Maryland) for providing GFP-tagged, U87 MG glioma cells; Mingxin Zhu for his assistance and expertise in cryosectioning of brains for the in vivo studies; Qian Li for her assistance with the injection of mice with GBM; and the Johns Hopkins University School of Medicine Microscope Facility for assistance in conducting electron microscopy imaging. C.L.S. was a recipient of the United Negro College Fund-Merck Science Initiative, Graduate Fellowship. Y.M.L. is a Howard Hughes Medical Research Fellow. The funders had no role in the study design, data collection and analysis, decision to publish, or preparation of the manuscript. A.Q.-H. was funded by NIH Grant RO1 NS070024 and the Howard Hughes Medical Institute. S.R.S. was supported by the National Science Foundation Graduate Research Fellowship. A.L. is currently affiliated with the Department of Biomedical Engineering, Yale University, New Haven, Connecticut, USA.

Author Contributions

C.L.S.: conception and design, study organization, design and construction of microfluidic devices for adherence experiments, design and construction of nanopatterned devices for migration experiments, performance of the experiments, data analysis and interpretation, manuscript writing; K.L.C.: performance of the experiments, data interpretation, manuscript writing; Y.M.L.: performance of the experiments, data analysis and interpretation, manuscript writing; B.L.: design and construction of microfluidic devices for chemotaxis experiments, performance of the experiments; K.M.S.: data analysis, manuscript writing; T.O. and S.G.: performance of the experiments, data analysis; S.R.S.: performance of the experiments; J.W.: design and construction of microfluidic devices for adherence experiments; O.W.: data analysis; M.D.: assistance with scanning electron microscopic imaging of devices and specimens; A.L. and A.Q.-H.: data interpretation, project supervision, manuscript writing.

Disclosure of Potential Conflicts of Interest

The authors indicated no potential conflicts of interest.

References

1 Ponte AL, Marais E, Gallay N et al. The in vitro migration capacity of human bone marrow mesenchymal stem cells: Comparison of chemokine and growth factor chemotactic activities. Stem Cells 2007;25:1737–1745.

2 Spaeth E, Klopp A, Dembinski J et al. Inflammation and tumor microenvironments: Defining the migratory itinerary of mesenchymal stem cells. Gene Ther 2008;15:730–738.

3 Karp JM, Leng Teo GS. Mesenchymal stem cell homing: The devil is in the details. Cell Stem Cell 2009;4:206–216.

4 Sordi V. Mesenchymal stem cell homing capacity. Transplantation 2009;87(suppl):S42–S45.

5 Yagi H, Soto-Gutierrez A, Parekkadan B et al. Mesenchymal stem cells: Mechanisms of immunomodulation and homing. Cell Transplant 2010;19:667–679.

6 Parekkadan B, Milwid JM. Mesenchymal stem cells as therapeutics. Annu Rev Biomed Eng 2010;12:87–117.

7 Kanehira M, Xin H, Hoshino K et al. Targeted delivery of NK4 to multiple lung tumors by bone marrow-derived mesenchymal stem cells. Cancer Gene Ther 2007;14:894–903.

8 Kidd S, Spaeth E, Dembinski JL et al. Direct evidence of mesenchymal stem cell tropism for tumor and wounding microenvironments using in vivo bioluminescent imaging. Stem Cells 2009;27:2614–2623.

9 Kosztowski T, Zaidi HA, Quiñones-Hinojosa A. Applications of neural and mesenchymal stem cells in the treatment of gliomas. Exp Rev Anticancer Ther 2009;9:597–612.

10 Zuk PA, Zhu M, Ashjian P et al. Human adipose tissue is a source of multipotent stem cells. Mol Biol Cell 2002;13:4279–4295.

11 Kucerova L, Matuskova M, Pastorakova A et al. Cytosine deaminase expressing human mesenchymal stem cells mediated tumour regression in melanoma bearing mice. J Gene Med 2008;10:1071–1082.

12 Chavakis E, Urbich C, Dimmeler S. Homing and engraftment of progenitor cells: A prerequisite for cell therapy. J Mol Cell Cardiol 2008;45:514–522.

13 Bexell D, Gunnarsson S, Tormin A et al. Bone marrow multipotent mesenchymal stroma cells act as pericyte-like migratory vehicles in experimental gliomas. Mol Ther 2009;17:183–190.

14 Kim SM, Lim JY, Park SI et al. Gene therapy using TRAIL-secreting human umbilical cord blood-derived mesenchymal stem cells against intracranial glioma. Cancer Res 2008;68:9614–9623.

15 Li Q, Wijesekera O, Salas SJ et al. Mesenchymal stem cells from human fat engineered to secrete BMP4 are nononcogenic, suppress brain cancer, and prolong survival. Clin Cancer Res 2014;20:2375–2387.

16 Sackstein R. The bone marrow is akin to skin: HCELL and the biology of hematopoietic

stem cell homing. J Investig Dermatol Symp Proc 2004;9:215–223.

17 Veevers-Lowe J, Ball SG, Shuttleworth A et al. Mesenchymal stem cell migration is regulated by fibronectin through $\alpha5\beta1$-integrin-mediated activation of PDGFR-β and potentiation of growth factor signals. J Cell Sci 2011;124:1288–1300.

18 Kulawig R, Krüger JP, Klein O et al. Identification of fibronectin as a major factor in human serum to recruit subchondral mesenchymal progenitor cells. Int J Biochem Cell Biol 2013;45: 1410–1418.

19 Pendleton C, Li Q, Chesler DA et al. Mesenchymal stem cells derived from adipose tissue vs bone marrow: In vitro comparison of their tropism towards gliomas. PLoS One 2013;8:e58198.

20 Stins MF, Gilles F, Kim KS. Selective expression of adhesion molecules on human brain microvascular endothelial cells. J Neuroimmunol 1997;76:81–90.

21 Gorelik M, Orukari I, Wang J et al. Use of MR cell tracking to evaluate targeting of glial precursor cells to inflammatory tissue by exploiting the very late antigen-4 docking receptor. Radiology 2012;265:175–185.

22 Shukaliak-Quandt J, Wong D, Dorovini-Zis K. Human brain microvessel endothelial cell and leukocyte interactions. Methods Mol Med 2003;89:337–348.

23 Garzon-Muvdi T, Schiapparelli P, ap Rhys C et al. Regulation of brain tumor dispersal by NKCC1 through a novel role in focal adhesion regulation. PLoS Biol 2012;10:e1001320.

24 Kim DH, Han K, Gupta K et al. Mechanosensitivity of fibroblast cell shape and movement to anisotropic substratum topography gradients. Biomaterials 2009;30:5433–5444.

25 Kim DH, Seo CH, Han K et al. Guided cell migration on microtextured substrates with variable local density and anisotropy. Adv Funct Mater 2009;19:1579–1586.

26 Lin B, Holmes WR, Wang CJ et al. Synthetic spatially graded Rac activation drives cell polarization and movement. Proc Natl Acad Sci USA 2012;109:E3668–E3677.

27 Dreger T, Watson JT, Akers W et al. Intravenous application of CD271-selected mesenchymal stem cells during fracture healing. J Orthop Trauma 2014;28(suppl 1):S15–S19.

28 Platten M, Kretz A, Naumann U et al. Monocyte chemoattractant protein-1 increases microglial infiltration and aggressiveness of gliomas. Ann Neurol 2003;54:388–392.

29 Kesanakurti D, Chetty C, Dinh DH et al. Role of MMP-2 in the regulation of IL-6/Stat3 survival signaling via interaction with $\alpha5\beta1$ integrin in glioma. Oncogene 2013;32:327–340.

30 Yamanaka R, Tanaka R, Saitoh T et al. Cytokine gene expression on glioma cell lines and specimens. J Neurooncol 1994;21:243–247.

31 Stamatovic SM, Keep RF, Kunkel SL et al. Potential role of MCP-1 in endothelial cell tight junction "opening": Signaling via Rho and Rho kinase. J Cell Sci 2003;116:4615–4628.

32 Flanagan LA, Rebaza LM, Derzic S et al. Regulation of human neural precursor cells by laminin and integrins. J Neurosci Res 2006;83: 845–856.

33 Porcionatto MA. The extracellular matrix provides directional cues for neuronal migration during cerebellar development. Braz J Med Biol Res 2006;39:313–320.

34 Bellail AC, Hunter SB, Brat DJ et al. Microregional extracellular matrix heterogeneity in brain modulates glioma cell invasion. Int J Biochem Cell Biol 2004;36:1046–1069.

35 Gonzalez-Perez O, Guerrero-Cazares H, Quiñones-Hinojosa A. Targeting of deep brain structures with microinjections for delivery of drugs, viral vectors, or cell transplants. J Vis Exp 2010;46:2082.

36 Choi SA, Hwang SK, Wang KC et al. Therapeutic efficacy and safety of TRAIL-producing human adipose tissue-derived mesenchymal stem cells against experimental brainstem glioma. Neuro Oncol 2011;13:61–69.

37 Lee DH, Ahn Y, Kim SU et al. Targeting rat brainstem glioma using human neural stem cells and human mesenchymal stem cells. Clin Cancer Res 2009;15:4925–4934.

38 Nakamura K, Ito Y, Kawano Y et al. Antitumor effect of genetically engineered mesenchymal stem cells in a rat glioma model. Gene Ther 2004;11:1155–1164.

39 Sasportas LS, Kasmieh R, Wakimoto H et al. Assessment of therapeutic efficacy and fate of engineered human mesenchymal stem cells for cancer therapy. Proc Natl Acad Sci USA 2009;106:4822–4827.

40 Cheng Z, Ou L, Zhou X et al. Targeted migration of mesenchymal stem cells modified with CXCR4 gene to infarcted myocardium improves cardiac performance. Mol Ther 2008;16:571–579.

41 Kim SM, Kim DS, Jeong CH et al. CXC chemokine receptor 1 enhances the ability of human umbilical cord blood-derived mesenchymal stem cells to migrate toward gliomas. Biochem Biophys Res Commun 2011;407:741–746.

42 Piccirillo SGM, Reynolds BA, Zanetti N et al. Bone morphogenetic proteins inhibit the tumorigenic potential of human brain tumour-initiating cells. Nature 2006;444:761–765.

43 Kumar S, Ponnazhagan S. Bone homing of mesenchymal stem cells by ectopic α 4 integrin expression. FASEB J 2007;21:3917–3927.

44 Zhang D, Fan GC, Zhou X et al. Overexpression of CXCR4 on mesenchymal stem cells augments myoangiogenesis in the infarcted myocardium. J Mol Cell Cardiol 2008; 44:281–292.

45 Yang B, Wu X, Mao Y et al. Dual-targeted antitumor effects against brainstem glioma by intravenous delivery of tumor necrosis factor-related, apoptosis-inducing, ligand-engineered human mesenchymal stem cells. Neurosurgery 2009;65:610–624.

See www.StemCellsTM.com for supporting information available online.

Pre-Exposure of Human Adipose Mesenchymal Stem Cells to Soluble Factors Enhances Their Homing to Brain Cancer

Chris L. Smith, Kaisorn L. Chaichana, Young M. Lee, Benjamin Lin, Kevin M. Stanko, Thomas O'Donnell, Saksham Gupta, Sagar R. Shah, Joanne Wang, Olindi Wijesekera, Michael Delannoy, Andre Levchenko and Alfredo Quiñones-Hinojosa

Stem Cells Trans Med 2015, 4:239-251.
doi: 10.5966/sctm.2014-0149 originally published online February 2, 2015